Tumor Vascular Maturation and Improved Drug Delivery Induced by Methylselenocysteine Leads to Therapeutic Synergy with Anticancer Drugs

Arup Bhattacharya,[1] Mukund Seshadri,[1,2] Steven D. Oven,[1] Károly Tóth,[1] Mary M. Vaughan,[3] and Youcef M. Rustum[1]

Abstract

Purpose: Our previously reported therapeutic synergy between naturally occurring seleno-amino acid methylselenocysteine (MSC) and anticancer drugs could not be shown *in vitro*. Studies were carried out to investigate the potential role of MSC-induced tumor vascular maturation and increased drug delivery in the observed therapeutic synergy *in vivo*.

Experimental Design: Mice bearing s.c. FaDu human head and neck squamous cell carcinoma xenografts were treated with MSC (0.2 mg/d × 14 days orally). Changes in microvessel density (CD31), vascular maturation (CD31/α-smooth muscle actin), perfusion (Hoechst 33342/$DiOC_7$), and permeability (dynamic contrast-enhanced magnetic resonance imaging) were determined at the end of the 14-day treatment period. Additionally, the effect of MSC on drug delivery was investigated by determining intratumoral concentration of doxorubicin using high-performance liquid chromatography and fluorescence microscopy.

Results: Double immunostaining of tumor sections revealed a marked reduction (~40%) in microvessel density accompanying tumor growth inhibition following MSC treatment along with a concomitant increase in the vascular maturation index (~30% > control) indicative of increased pericyte coverage of microvessels. Hoechst 33342/$DiOC_7$ staining showed improved vessel functionality, and dynamic contrast-enhanced magnetic resonance imaging using the intravascular contrast agent, albumin-GdDTPA, revealed a significant reduction in vascular permeability following MSC treatment. Consistent with these observations, a 4-fold increase in intratumoral doxorubicin levels was observed with MSC pretreatment compared with administration of doxorubicin alone.

Conclusion: These results show, for the first time, the antiangiogenic effects of MSC results in tumor growth inhibition, vascular maturation *in vivo*, and enhanced anticancer drug delivery that are associated with the observed therapeutic synergy *in vivo*.

Selenium is an essential trace element present in grains, meat, yeast, and vegetables with an average nutritional intake of 50 to 350 μg/d (1). A strong inverse association between selenium status and site- and sex-specific cancer mortality rates for cancers of the lung, bladder, esophagus, and breast has been reported (1, 2). Although the use of selenium as a chemopreventive agent has been a subject of research for decades, its activity as a therapeutic agent has not been extensively investigated. We have been investigating the antitumor activity of selenium alone and in combination with chemotherapy in preclinical and clinical settings (3, 4). We have shown previously that selenium administered in its organic form as methylselenocysteine (MSC) significantly potentiates efficacy of the topoisomerase I inhibitor, irinotecan (Camptosar), against human tumor xenografts (3). Similar effects were seen with docetaxel, cisplatin, and oxaliplatin in a variety of drug-sensitive and drug-resistant human tumor xenografts. However, the mechanism(s) that contribute to the observed therapeutic synergy are not completely clear. Recent studies in our laboratory have revealed down-regulation of proangiogenic growth factors, cyclooxygenase-2, nitric oxide synthase, and hypoxia-inducible factor-1α expression in human head and neck squamous cell carcinoma (HNSCC; FaDu) xenografts with combination treatment (5). Studies carried out in our laboratory using FaDu tumor cells revealed only additive effects *in vitro*,[4] further implicating tumor vasculature in the observed enhancement of antitumor activity.

Authors' Affiliations: Departments of [1]Cancer Biology, [2]Preclinical Imaging Resource, and [3]Pathology and Laboratory Medicine, Roswell Park Cancer Institute, Buffalo, New York

Received 1/25/08; revised 3/5/08; accepted 3/11/08.

Grant support: American Institute for Cancer Research grant 06A072 (A. Bhattacharya) and National Cancer Institute Comprehensive Cancer Center Support Grant CA016056.

The costs of publication of this article were defrayed in part by the payment of page charges. This article must therefore be hereby marked *advertisement* in accordance with 18 U.S.C. Section 1734 solely to indicate this fact.

Note: A. Bhattacharya and M. Seshadri contributed equally to this work.

Requests for reprints: Arup Bhattacharya, Department of Cancer Biology, Roswell Park Cancer Institute, Elm and Carlton Streets, Buffalo, NY 14263. Phone: 716-845-4944; Fax: 716-845-4928; E-mail: arup.bhattacharya@roswellpark.org.

doi:10.1158/1078-0432.CCR-08-0212

[4] Y.M. Rustum, unpublished observation.

Angiogenesis is an early event in tumor progression and is critical for continued growth of solid tumors beyond a few millimeters (6). It is now widely acknowledged that inhibiting the angiogenic process is an effective way of controlling tumor growth, and to this end, several antiangiogenic agents are currently undergoing preclinical and clinical evaluation (7). Selenium has also been shown to exhibit antiangiogenic properties *in vitro* and *in vivo* (8, 9). Studies carried out in human umbilical vein endothelial cells have shown induction of cell death through apoptosis and reduction in matrix metalloproteinase activity (8). Selenium intake, in the form of selenized garlic or MSC has also been shown to result in reduction of vascular endothelial growth factor levels in mammary carcinomas (9). However, the effects of selenium on tumor vascular maturation and blood flow have not been previously investigated.

Therefore, in this study, we examined the effect of MSC on several phenotypic and functional variables related to tumor angiogenesis *in vivo*. Using s.c. FaDu human tumor xenografts implanted in nude mice, changes in microvessel density (MVD), pericyte coverage [vascular maturation index (VMI)], vascular perfusion, permeability, and tumor growth were evaluated following MSC treatment (0.2 mg/d × 14 days). Additionally, the effect of MSC treatment on intratumoral drug delivery and distribution was investigated using the autofluorescent anthracycline doxorubicin. The results obtained show, for the first time, that administration of nontoxic dose of selenium, daily for 14 days results in a marked inhibition of angiogenesis, tumor growth inhibition while concomitantly improving vascular function, and therapeutic delivery and distribution of the drug into the tumor.

Materials and Methods

Tumor model. The human HNSCC cell line FaDu was originally purchased from American Type Culture Collection and xenografts were established in 6- to 8-week-old female athymic nude mice (Foxn1^{nu}, Harlan-Sprague-Dawley) as described previously (3). Tumor growth following treatment was measured (n = 6 per group) using Vernier calipers and tumor volumes were calculated (3). All studies were done in accordance with protocols approved by the Institute Animal Care and Use Committee at Roswell Park Cancer Institute.

Drugs. MSC (Sigma) was dissolved in sterile saline at a concentration of 1 mg/mL and administered orally at the maximum tolerated dose of 0.2 mg/mouse/d (3) for 14 days, beginning 4 days after tumor implantation. For drug delivery studies, doxorubicin (Bedford Laboratories) was administered i.v. (30 mg/kg) alone or 24 h following administration of the last MSC dose (day 14).

Immunohistochemistry. Immunohistochemical staining for endothelial cells and pericytes was done using CD31 and α-smooth muscle actin (α-SMA), respectively. We have described previously procedures for CD31 immunostaining of tumor sections in detail (10). For CD31/α-SMA double staining, 5 to 8 μm cryosections were fixed in cold acetone (-20°C) for 15 min followed by a rinse in PBS with 0.05% Tween 20. Endogenous peroxidase quenching was followed by incubation with rabbit polyclonal α-SMA antibody (1 μg/mL or 1:500; Abcam) and biotinylated goat anti-rabbit secondary antibody (1:250; Vector Laboratories) for 30 min. This was followed by streptavidin complex (Zymed Laboratories) for 30 min and chromogen 3,3-diaminobenzidine (DAKO) for 5 min. Again, a blocking step with 0.03% casein was used followed by CD31 antibody (BD Biosciences PharMingen) at 10 μg/mL for 60 min. Biotinylated anti-rat secondary antibody (BD Biosciences PharMingen) at 1:100 was used for 30 min followed by alkaline phosphatase (DAKO)–conjugated streptavidin reagent for 25 min. The chromogen Fast Red was then applied for 10 min and the slides were counterstained with Mayer's hematoxylin (DAKO) for 45 s. An isotype-matched rat IgG was used as a negative control. Endothelial cells were immunostained red and pericytes were stained brown. There were a minimum of five tumors per group and three sections from each tumor at least 10 μm apart were used for quantification purposes.

Dynamic contrast-enhanced magnetic resonance imaging. To determine MSC-induced changes in vascular permeability, dynamic contrast-enhanced magnetic resonance imaging using the intravascular contrast agent, albumin-GdDTPA, was done in a 4.7T/33 cm horizontal bore MR scanner (GE Instruments) on a separate cohort of mice (n = 4 per group). Before imaging, animals were anesthetized using ketamine/xylazine mixture (10:1) at a dose of 1.0 mL/100 g and positioned in the scanner. We have described previously the imaging protocol for calculating changes in vascular permeability (11). Briefly, the T1 relaxation rate of tissue (R1 = 1 / T1) increases linearly with contrast agent concentration. We therefore acquired serial T1-weighted images before and after contrast agent administration using a saturation recovery, fast spin echo sequence with an effective time of echo period = 10 ms and repetition time ranging from 360 to 6,000 ms (field of view = 32 × 32 mm, slice thickness = 1.0 mm, matrix size = 128 × 96 pixels, number of excitations = 3) to determine the change in T1 relaxation rates (ΔR1) of different tissues (tumor, muscle, and kidneys). Applying a linear regression analysis to the change in ΔR1 over time, we can acquire both a slope and a γ intercept. The slope is a measure of vascular permeability and the γ intercept of the slope (at time 0; that is, immediately after administration of the contrast agent) is a measure of vascular volume (11).

Determination of vessel functionality. To determine the effect of MSC on vessel functionality, the double-fluorescent dye technique based on the perfusion markers, Hoechst 33342 (Sigma) and $DiOC_7$ (Molecular Probes), were used on a separate cohort of mice (n = 4). The different fluorescence excitation and emission properties of the two dyes allow for detection of temporal and spatial fluctuations in perfusion (12, 13). The experimental details of the technique have been published previously (12, 13). Briefly, the fluorescent dyes were administered i.v. (Hoechst 33342, 15 mg/kg; $DiOC_7$, 1 mg/kg) separated by a 20-min interval and tumors were excised 5 min after the second $DiOC_7$ injection. Cryosections (5-10 μm thick) of the tumor were used for fluorescence detection of Hoechst 33342 and $DiOC_7$ using ×10 objective of Leica confocal microscope (Leica Microsystem Heidelberg GmbH) with excitation at 488 nm and emission at 500 to 700 nm.

Determination of doxorubicin concentration and distribution. The effect of MSC on drug delivery (n = 11 per group) and distribution (n = 105 linear paths using 24 different sections from 4 different tumors per group) was assessed using high-performance liquid chromatography (HPLC; ref. 14) and fluorescence microscopy (15). Doxorubicin was given at a dose of 30 mg/kg to facilitate detection and quantification of autofluorescence (15). For HPLC, the separation method was carried out on a Waters Nova-Pak C18 column equipped with Bondapak C18 guard column, with mobile phase consisting of 20% acetonitrile and 80% triethylamine acetate. The detection was by fluorescence, with excitation at 370 nm and emission at 510 nm as described previously (14). In addition to the tumor, doxorubicin concentration was determined in normal tissues, liver, kidney, and small intestines from animals treated with doxorubicin alone or MSC plus doxorubicin. For fluorescence microscopy, 2 h after doxorubicin administration, animals were euthanized and ~5 to 10 μm thick frozen sections were used. An average of four maximum intensity projection images with a resolution of 0.23 μm were acquired under the ×63 objective of Leica confocal microscope similar to procedures described previously (15). All images were obtained and digitized using identical acquisition variables.

Image analysis. MVD counts were determined by counting $CD31^+$ endothelial cell clusters in multiple high-power fields (×400) covering nonnecrotic areas of the whole tumor. For determination of vessel lumen area, photomicrographs of CD31-stained sections (×400) were digitized at 1,350 dpi and areas were manually segmented using the region-of-interest module of the medical imaging software, Analyze (AnalyzeDirect). The VMI was derived by calculating the total number of $CD31^+$ α-SMA^+ areas and areas positive for CD31 alone in double-stained (CD31/α-SMA) tissue sections using Analyze (16). For drug delivery studies, the mean intensity of doxorubicin autofluorescence at various distances away from the blood vessels was calculated using Analyze. At least three tumors for each group were analyzed for MVD, vessel lumen, VMI, and doxorubicin studies.

Statistical analysis. All results are reported as mean ± SE. Differences between the mean of the groups were analyzed using unpaired two-tailed Student's *t* test (GraphPad version 4.00; GraphPad Software). *P* values < 0.05 were considered statistically significant.

Results

MSC lowers tumor MVD. As shown in Fig. 1A, treatment with MSC (0.2 mg/mouse/d) for 14 days resulted in ~40% reduction in MVD (13.56 ± 4.875; $P = 0.02$) compared with untreated control tumors (21.26 ± 1.52). This effect was tumor specific with no significant change in MVD observed in normal mouse liver tissue (Fig. 1A). Quantitative measurements of vessel size in CD31-immunostained tumor sections showed a significant reduction in vessel lumen area following MSC treatment (Fig. 1B; $P = 0.0009$).

MSC causes tumor growth inhibition. To determine the effect of MSC treatment (0.2 mg/mouse/d) for 14 days on tumor growth, changes in tumor volume were calculated for a period of 30 days following treatment. As shown in Fig. 1C, a marked reduction ($P = 0.002$) in tumor growth was observed following MSC treatment compared with untreated controls.

MSC induces tumor vascular maturation. As shown in Fig. 2A, double-stained sections of FaDu tumors obtained from mice treated with MSC showed increased α-SMA staining compared with untreated controls. The VMI, percentage of endothelial cells associated with pericytes, is used as a quantitative measure of vascular maturation (16–18). Quantitative analysis of pericyte coverage showed ~30% increase in VMI in MSC-treated FaDu tumors compared with control FaDu tumors (Fig. 2B). Comparative analysis of VMI in normal liver tissue did not reveal any change in pericyte coverage, indicating the selectivity of MSC-induced changes in vascular maturation.

MSC reduces tumor vascular leakiness. The functional consequences of MSC-induced changes in MVD and VMI on vascular permeability in FaDu xenografts following MSC treatment were assessed using noninvasive dynamic contrast-enhanced magnetic resonance imaging. As shown in Fig. 2C, dynamic contrast-enhanced magnetic resonance imaging of untreated FaDu tumors showed increase (slope, 0.0062 ± 0.001; $r^2 = 0.7999$) in the longitudinal relaxation rate (ΔR1) as function of time following administration of the intravascular magnetic resonance contrast agent, albumin-GdDTPA, indicative of significant vascular leakiness. Consistent with the results of MVD and VMI studies, linear regression analysis of ΔR1 over time in MSC-treated animals revealed a marked reduction in tumor vascular permeability (slope, 0.00023 ± 0.0004; $r^2 = 0.097$; $P = 0.0147$) compared with untreated controls, a sign of improved tumor vascular normalization.

MSC improves tumor vascular function. We assessed fluctuations in blood flow in untreated controls and MSC-treated FaDu tumors using the double-fluorescent dye method (12, 13) based on two perfusion markers, Hoechst 33342 and $DiOC_7$. Using this technique, studies have shown previously that

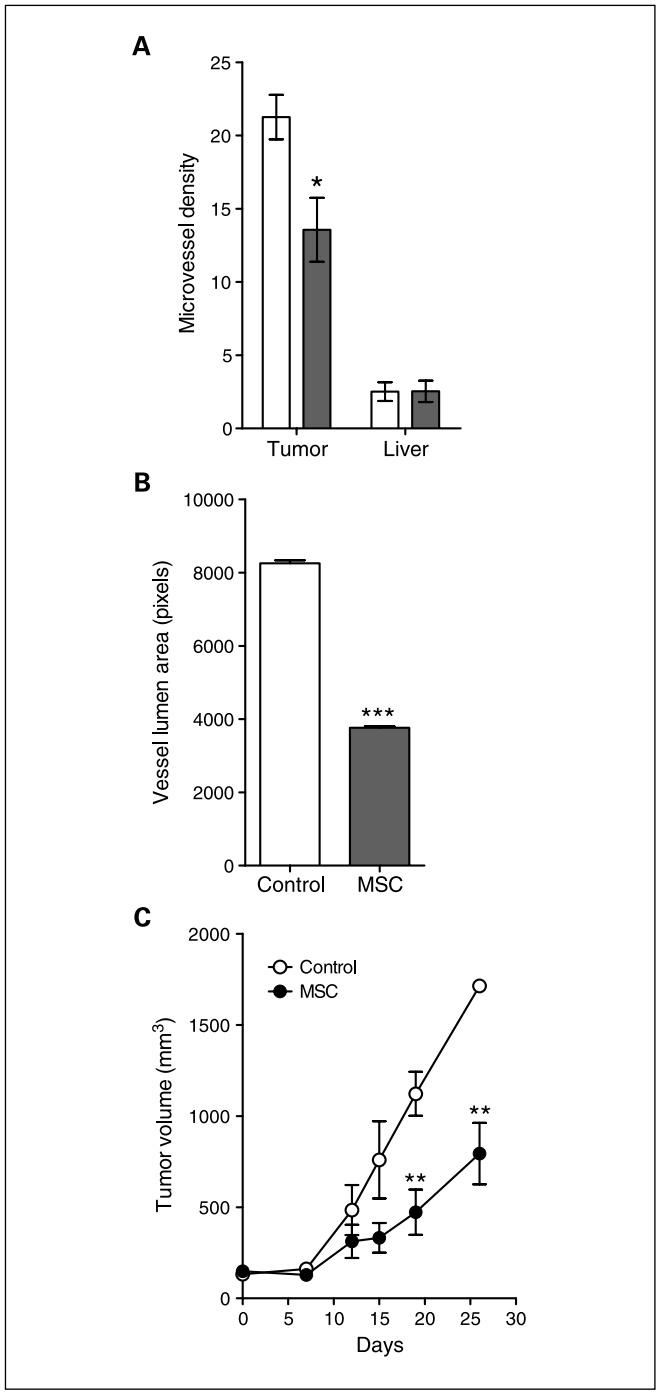

Fig. 1. Effect of 14 d of MSC treatment on MVD and growth of HNSCC xenografts. *A,* MVD in untreated controls and MSC-treated FaDu tumors following 14 d of MSC treatment (0.2 mg/mouse/d). MVD counts per high-power field (*HPF*). Original magnification, ×400. Significant reduction in MVD was seen after 14 d of MSC treatment in tumors, but no change was seen in liver. *B,* quantitation of vessel lumen area in control and MSC-treated FaDu xenografts from CD31-immunostained tumor sections. *C,* change in median tumor volume between MSC-treated tumors and untreated controls over a 30-d period following treatment. ***, $P < 0.001$; **, $P < 0.01$; *, $P < 0.05$, two-tailed Student's *t* test.

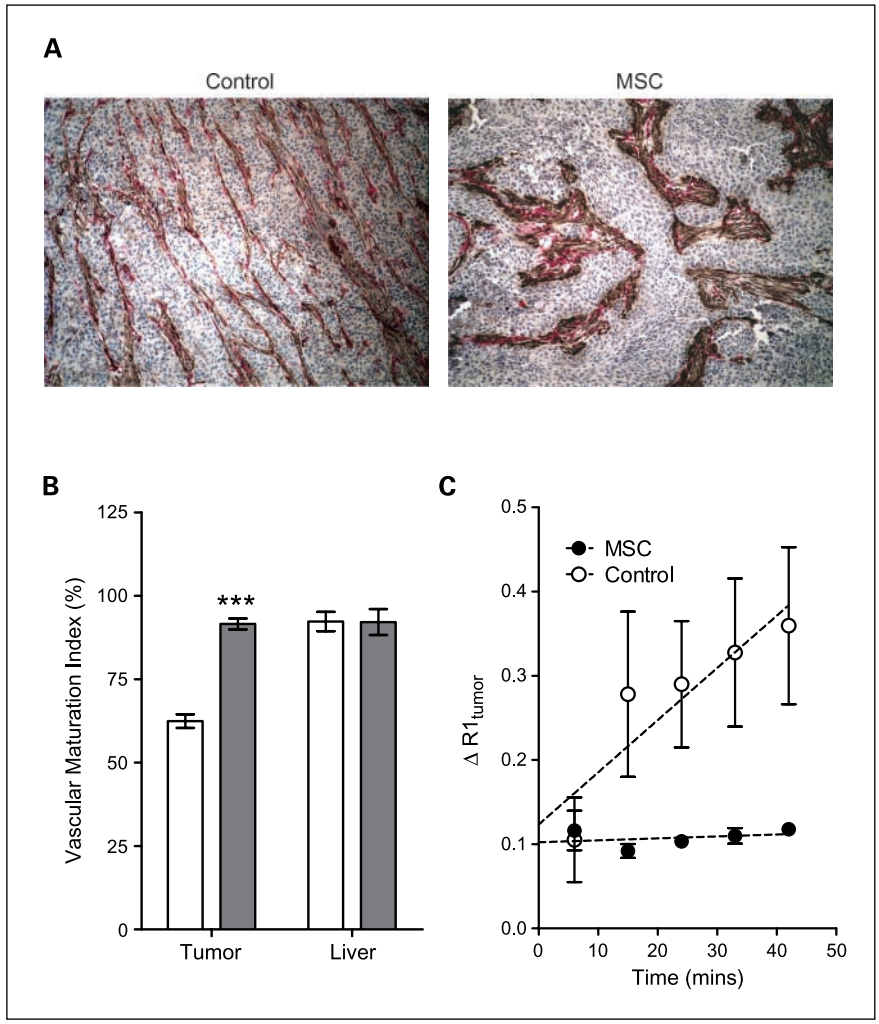

Fig. 2. Effect of MSC treatment on vascular maturation, permeability, and function in HNSCC xenografts. *A,* photomicrographs of double-stained (CD31/α-SMA) section of a MSC-treated FaDu tumor (*right* magnification, ×400) showing increased pericytes (*brown*) associated with blood vessels (*red*) compared with the image of an untreated control FaDu tumor (*left*). *B,* quantitative estimates of VMI in untreated controls (*white columns*) and MSC-treated FaDu tumors (*gray columns*). VMI analysis was also done on mouse liver as normal tissue control. *C,* change in T1 relaxation rates (ΔR1) over time of untreated controls (*white circles*) and tumors treated with MSC (*dark circles*). Linear regression analysis of the slopes of ΔR1 values for control and MSC-treated tumors revealed a significant reduction in permeability following treatment ($P = 0.017$). ***, $P < 0.001$, two-tailed Student's *t* test.

vessels that experience intermittent flow show uptake of only one dye ("mismatched" vessels; refs. 12, 13). Fluorescence microscopy revealed minimal uptake of both dyes in control FaDu tumors, with a majority of these perfused vessels observed in the tumor periphery (Fig. 3A). In contrast, MSC-treated tumors showed uniform uptake of both dyes indicative of improved vessel functionality.

MSC enhances tumor drug delivery. HPLC analysis (Fig. 3B) revealed a 4-fold increase in doxorubicin concentration in MSC-treated FaDu tumors (0.62 ± 0.16 μg; $P = 0.01$) compared with untreated controls (0.16 ± 0.03 μg). No significant change was seen in the plasma and normal tissue (kidneys, liver, and small intestine) levels of doxorubicin in both cohorts of mice. Visualization and quantitation of doxorubicin levels using fluorescence also showed increased intensity at regions close to the vessel wall and away from the blood vessel (*blue arrows*), highlighting the improvement in both delivery and penetration of doxorubicin following MSC treatment (Fig. 3C and D).

Discussion

We have shown previously that administration of MSC for a period of 7 days before irinotecan treatment significantly enhances long-term cure rates in mice bearing s.c. FaDu tumors (3). Similar therapeutic synergy with MSC was seen with different chemotherapeutic drugs (e.g., Taxol, taxotere, doxorubicin, cisplatin, and oxaliplatin) and in different human xenografts growing in nude mice.[4] However, in contrast to the impressive therapeutic synergy observed *in vivo*, only additive effects were observed *in vitro*. Based on these observations, we hypothesized that tumor vasculature was a potential target of action of MSC and the antiangiogenic and vessel normalization activity of MSC was responsible at least in part for the observed therapeutic synergy. To test this hypothesis, studies were done to determine the vascular phenotypic and functional effects of MSC *in vivo* using autofluorescent anticancer drug doxorubicin. These studies were aimed at understanding the mechanism(s) that contribute to the observed therapeutic synergy with selenium and chemotherapy.

First, we examined the effects of MSC on MVD and vessel lumen area using immunohistochemistry. Treatment with MSC (0.2 mg/mouse/d) for 14 days resulted in a significant reduction in MVD ($P = 0.02$) compared with untreated control tumors (Fig. 1A). No change was seen in normal mouse liver tissue MVD (Fig. 1A), indicating thereby that the antiangiogenic effect is tumor specific and a contributing factor in significantly delaying tumor growth (Fig. 1C).

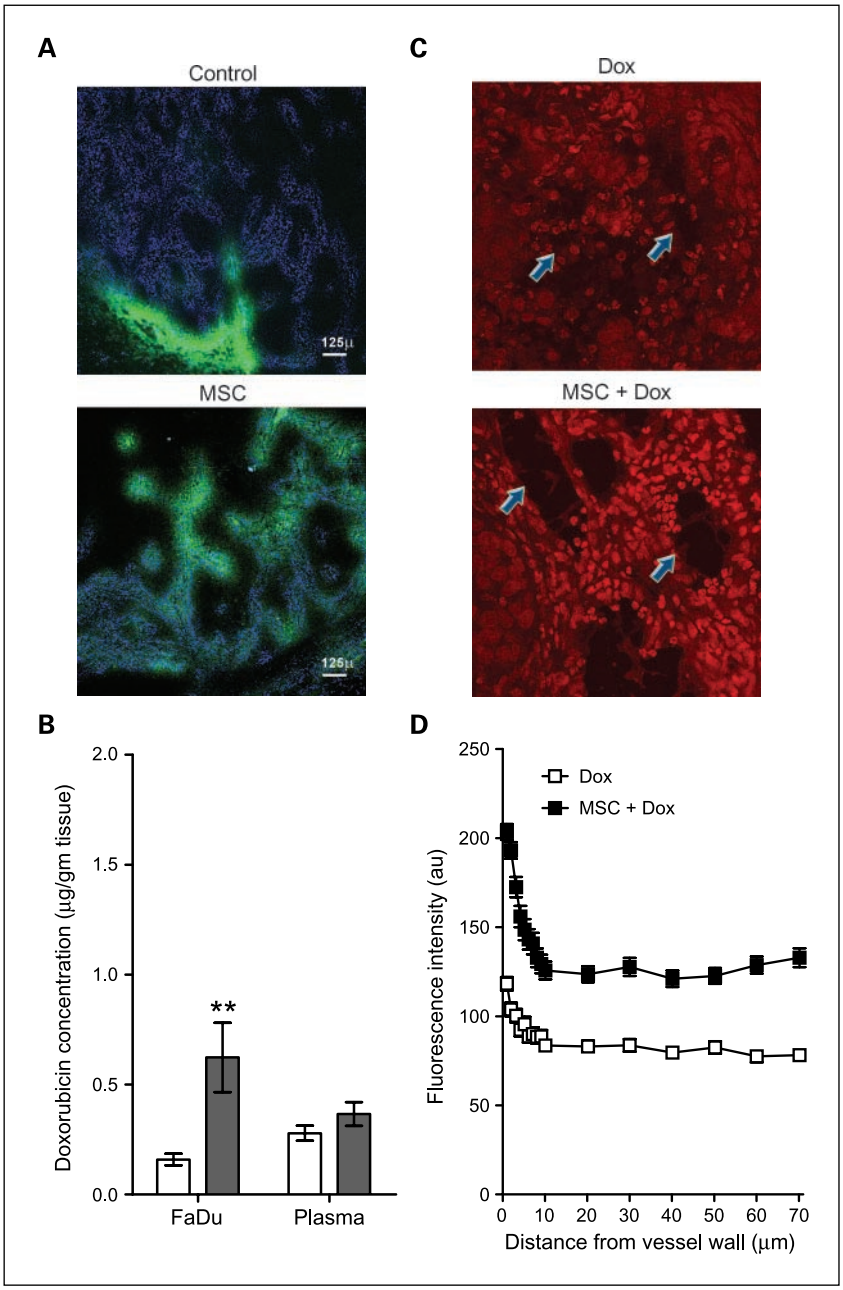

Fig. 3. Effect of MSC treatment on drug delivery. *A,* visualization of fluctuations in vessel perfusion was done using the double-fluorescent dye method (described in Materials and Methods). Fluorescence microscopic images of control and MSC-treated FaDu tumors following administration of the perfusion markers, Hoechst 33342 (*blue*) and $DiOC_7$ (*green*). Note uniform uptake of both fluorescent dyes in MSC-treated tumors (*bottom*) compared with untreated controls. *B,* HPLC-based determination of doxorubicin concentration in FaDu tumors following administration of either doxorubicin alone (*white columns*) or MSC plus doxorubicin (*gray columns*). A 4-fold increase in doxorubicin concentration was found in FaDu tumors with MSC pretreatment. No significant change in doxorubicin concentration was observed in plasma. *C,* corresponding representative fluorescence images (×630) obtained from FaDu tumors (*arrows,* vessels) in mice treated with doxorubicin alone (*Dox*) and MSC plus doxorubicin (*MSC+Dox*), showing higher fluorescence after combination treatment. *D,* quantitation of doxorubicin fluorescence intensity (*au*) in tumors treated with doxorubicin with MSC and without MSC. Pretreatment with MSC showing improved delivery and penetration of doxorubicin with combination treatment. ***, $P < 0.001$, two-tailed Student's *t* test.

Tumor vasculature has an important role in the pathophysiology of solid tumors including tumor growth, invasion, metastasis, and response to therapies. The hallmark of tumor vasculature is the morphologically abnormal vascular architecture consisting of chaotic, dilated vessels showing poor overall perfusion that resists blood flow and drug delivery in tumors. These functional characteristics of tumor vasculature contribute to an elevated tumor interstitial fluid pressure that opposes diffusion and convection—the main form of transvascular transport of therapeutic agents in tumors (19). Thus, delivery of therapeutic agents both across the blood vessel wall and interstitium is compromised in solid tumors (19). In contrast to the vasculature seen in normal tissues, tumor endothelium lacks the support of pericytes, cells that serve to stabilize blood vessels and stimulate basement membrane production (20). Recent preclinical studies using antiangiogenic agents such as bevacizumab and DC101 have shown that in addition to potent effects on tumor vascular morphology (vessel size and density), these agents also cause decrease in leakiness and increased maturation of tumor vasculature through increased recruitment of pericytes to the vascular bed (17, 18). Pericytes express α-SMA, immunostaining of which is widely used as a marker for pericyte coverage in tissue sections (16–18). The VMI, percentage of endothelial cells associated with pericytes, is used as a quantitative measure of vascular maturation (16–18). Quantitative analysis of pericyte coverage showed ~30% increase in VMI in MSC-treated FaDu tumors compared with control FaDu tumors (Fig. 2B). Comparative analysis of VMI in normal liver tissue did not reveal any change in pericyte coverage, indicating the selectivity of MSC-induced changes in tumor vascular maturation. The structural aberrations associated with tumor vasculature contribute to significant

functional abnormalities including enhanced vascular permeability and temporal and spatial variations in blood flow, factors that are detrimental to tumor drug delivery and distribution (6, 20). Previous studies have shown that inhibition of vascular endothelial growth factor can result in pruning of immature vessels while contributing to the evolution of a more mature vascular phenotype, typically characterized by reduced permeability and increased perfusion. This decreases tumor interstitial fluid pressure and restores the pressure gradient across blood vessel wall as well as tumor interstitium leading to a better tumor drug delivery and penetration (18, 19, 21). To determine if a similar phenomenon was occurring with MSC and to assess the functional consequences of MSC-induced changes in MVD and VMI, dynamic contrast-enhanced magnetic resonance imaging was used as a noninvasive tool to assess changes in vascular permeability in FaDu xenografts following MSC treatment. Consistent with the results of MVD and VMI studies, linear regression analysis (Fig. 2C) of longitudinal relaxation rate ($\Delta R1$) as function of time following administration of the intravascular magnetic resonance contrast agent, albumin-GdDTPA, in MSC-treated animals revealed a marked reduction in tumor vascular permeability (slope, 0.00023 ± 0.0004; $r^2 = 0.097$; $P = 0.0147$) compared with untreated controls (slope, 0.0062 ± 0.001; $r^2 = 0.7999$). Reduction in tumor vascular leakiness is a hallmark of tumor vascular normalization.

Finally, it has been shown that the "normalization" process induced by antiangiogenic therapy would, at least transiently, improve functionality of blood vessels enhancing drug delivery to tumors (17, 18, 21). We therefore evaluated if pretreatment with MSC resulted in a similar improvement in perfusion and drug delivery. We first assessed fluctuations in blood flow in untreated controls and MSC-treated FaDu tumors using the double-fluorescent dye method (12, 13) based on two perfusion markers, Hoechst 33342 and $DiOC_7$. Using this technique, studies have shown previously that vessels that experience intermittent flow show uptake of only one dye ("mismatched" vessels; refs. 12, 13). In our study, tumors treated with MSC showed an improved tumor vessel functionality indicated by uptake of both dyes, whereas in control FaDu tumors a majority of these perfused vessels were observed only in the tumor periphery (Fig. 3A). Consistent with these observations, HPLC analysis (Fig. 3B) revealed a 4-fold increase in doxorubicin concentration in MSC-treated FaDu tumors (0.62 ± 0.16 μg; $P = 0.01$) compared with untreated controls (0.16 ± 0.03 μg). No significant change was seen in the plasma and normal tissue (kidneys, liver, and small intestine) levels of doxorubicin in both cohorts of mice. Visualization and quantitation of doxorubicin levels using fluorescence also showed increased intensity at regions close to the vessel wall and away from the blood vessel (*blue arrows*), highlighting the improvement in both intratumoral delivery and penetration of doxorubicin following MSC treatment (Fig. 3C and D).

In conclusion, the results of our studies have shown, for the first time, potent effects of MSC on tumor angiogenesis and vascular maturation, which resulted in improved vascular function and drug delivery in HNSCC xenografts. Similar results were seen with another HNSCC xenograft A253 (data not shown). It is likely that changes in the tumor microenvironment initiated by MSC-induced tumor vascular maturation play a critical role in the reported (3) potentiation of chemotherapeutic efficacy in preclinical models. Consistent with the findings of this report, ongoing studies have revealed a 34% reduction in interstitial fluid pressure following MSC treatment in FaDu tumors (5.58 ± 0.83 mm Hg; $P = 0.025$) compared with untreated controls (8.87 ± 0.961 mm Hg) and measurements of pO_2 levels showed increased oxygenation in MSC-treated FaDu tumors compared with controls (2.864 ± 0.18 versus 1.66 ± 0.24; $P = 0.01$),[5] consistent with our recent observation of synergy between selenium and radiation therapy (22). A decrease in tumor interstitial fluid pressure improves delivery and penetration of therapeutics by restoring the pressure gradient across blood vessel wall as well as tumor interstitium (19, 21).

Although the focus on selenium in the past has been mainly for its chemopreventive properties, its use as a biological agent sensitizing tumor to subsequent treatment with anticancer drugs in advanced cancers *in vivo* is of recent origin. The use of organo-selenium compound selenomethionine as a suicide prodrug substrate for conversion to its active metabolite methylselenol through methioninase-based cancer gene therapy has been reported earlier with encouraging results in preclinical animal models (23). In contrast, our study provides evidence for use of MSC as an antiangiogenic agent that has limited tumor growth inhibition but can normalize tumor vasculature and microenvironment and thus enhance the therapeutic efficacy of a wide variety of anticancer agents when used in combination therapy. Selenium, a constituent of mammalian physiology, is well tolerated and results in preclinical model systems strongly support its role as a modulator of antitumor activity and toxicity of chemotherapy (3). Although the selenium dose used in this study is considerably higher than the daily dose of 200 μg used in chemoprevention trials, a recent phase I study conducted at Roswell Park Cancer Institute has shown that selenium is well tolerated at relatively high doses (7,200 μg) over long periods in humans without serious adverse effects (24, 25). At this dose, the achievable plasma selenium levels are equivalent to those observed in the preclinical model system. Overall, the results of this study provide useful information for future trial design and evaluation of combination strategies involving the use of high nontoxic doses of selenium in combination with chemotherapy and radiotherapy.

Disclosure of Potential Conflicts of Interest

No potential conflicts of interest were disclosed.

Acknowledgments

We thank Dr. Lakshmi Pendyala for assistance with the HPLC quantitation and Ed Hurley for assistance with fluorescence microscopy.

[5] A. Bhattacharya, personal communication.

References

1. Combs GF, Jr., Gray WP. Chemopreventive agents: selenium. Pharmacol Ther 1998;79:179–92.
2. Clark LC, Combs GF, Jr., Turnbull BW, et al. Effects of selenium supplementation for cancer prevention in patients with carcinoma of the skin. A randomized controlled trial. Nutritional Prevention of Cancer Study Group. JAMA 1996;276:1957–63.
3. Cao S, Durrani FA, Rustum YM. Selective modulation

of the therapeutic efficacy of anticancer drugs by selenium containing compounds against human tumor xenografts. Clin Cancer Res 2004;10:2561–9.

4. Fakih MG, Pendyala L, Smith PF, et al. A phase I and pharmacokinetic study of fixed-dose selenomethionine and irinotecan in solid tumors. Clin Cancer Res 2006;12:1237–44.

5. Yin MB, Li ZR, Toth K, et al. Potentiation of irinotecan sensitivity by Se-methylselenocysteine in an *in vivo* tumor model is associated with downregulation of cyclooxygenase-2, inducible nitric oxide synthase, and hypoxia-inducible factor 1α expression, resulting in reduced angiogenesis. Oncogene 2006; 25:2509–19.

6. Folkman J. Tumor angiogenesis: therapeutic implications. N Engl J Med 1971;285:1182–6.

7. Cristofanilli M, Charnsangavej C, Hortobagyi GN. Angiogenesis modulation in cancer research: novel clinical approaches. Nat Rev 2002;1:415–26.

8. Jiang C, Ganther H, Lu J. Monomethyl selenium-specific inhibition of MMP-2 and VEGF expression: implications for angiogenic switch regulation. Mol Carcinog 2000;29:236–50.

9. Jiang C, Jiang W, Ip C, Ganther H, Lu J. Selenium-induced inhibition of angiogenesis in mammary cancer at chemopreventive levels of intake. Mol Carcinog 1999;26:213–25.

10. Bhattacharya A, Toth K, Mazurchuk R, et al. Lack of microvessels in well-differentiated regions of human head and neck squamous cell carcinoma A253 associated with functional magnetic resonance imaging detectable hypoxia, limited drug delivery, and resistance to irinotecan therapy. Clin Cancer Res 2004;10: 8005–17.

11. Seshadri M, Mazurchuk R, Spernyak JA, Bhattacharya A, Rustum YM, Bellnier DA. Activity of the vascular-disrupting agent 5,6-dimethylxanthenone-4-acetic acid against human head and neck carcinoma xenografts. Neoplasia 2006;8:534–42.

12. Olive PL. Radiation-induced reoxygenation in the SCCVII murine tumour: evidence for a decrease in oxygen consumption and an increase in tumour perfusion. Radiother Oncol 1994;32:37–46.

13. Trotter MJ, Chaplin DJ, Olive PL. Use of a carbocyanine dye as a marker of functional vasculature in murine tumours. Br J Cancer 1989;59:706–9.

14. Warner DL, Burke TG. Simple and versatile high-performance liquid chromatographic method for the simultaneous quantitation of the lactone and carboxylate forms of camptothecin anticancer drugs. J Chromatography B 1997;691:161–71.

15. Primeau AJ, Rendon A, Hedley D, Lilge L, Tannock IF. The distribution of the anticancer drug doxorubicin in relation to blood vessels in solid tumors. Clin Cancer Res 2005;11:8782–8.

16. Kakolyris S, Giatromanolaki A, Koukourakis M, et al. Assessment of vascular maturation in non-small cell lung cancer using a novel basement membrane component, LH39: correlation with p53 and angiogenic factor expression. Cancer Res 1999;59:5602–7.

17. Dickson PV, Hamner JB, Sims TL, et al. Bevacizumab-induced transient remodeling of the vasculature in neuroblastoma xenografts results in improved delivery and efficacy of systemically administered chemotherapy. Clin Cancer Res 2007;13: 3942–50.

18. Tong R, Boucher Y, Kozin S, Winkler F, Hicklin D, Jain R. Vascular normalization by vascular endothelial growth factor receptor 2 blockade induces a pressure gradient across the vasculature and improves drug penetration in tumors. Cancer Res 2004;64: 3731–6.

19. Fukumura D, Jain RK. Tumor microvasculature and microenvironment: targets for anti-angiogenesis and normalization. Microvasc Res 2007;74:72–84.

20. Ruoslahti E. Specialization of tumour vasculature. Nat Rev Cancer 2002;2:83–90.

21. Jain RK. Normalizing tumor vasculature with anti-angiogenic therapy: a new paradigm for combination therapy. Nature Med 2001;7:987–9.

22. Durrani F, Cao S, Park Y, et al. Synergistic effect of selenium compounds with radiation therapy in human A549 lung xenografts [abstract 750]. Proc AACR 2007.

23. Miki K, Xu M, Gupta A, et al. Methioninase cancer gene therapy with selenomethionine as suicide prodrug substrate. Cancer Res 2001;61:6805–10.

24. Fakih M, Pendyala L, Brady W, et al. A phase I and pharmacokinetic study of selenomethionine in combination with a fixed dose of irinotecan in solid tumors. Cancer Chemother Pharmacol 2007; DOI 10.1007/s00280-007-0631-4.

25. Rustum Y, Pendyala L, Creaven P, et al. A phase I dose escalation study of selenomethionine (SLM) in combination with fixed dose irinotecan in patients with solid tumors. J Clin Oncol 2007;25:115S.